PAPER

The half-sandwich 18- and 16-electron arene ruthenium iminophosphonamide complexes†

Tat'yana A. Peganova,[a] Iana S. Sinopalnikova,[a] Alexander S. Peregudov,[a] Ivan V. Fedyanin,[a] Albert Demonceau,[b] Nikolai A. Ustynyuk[a] and Alexander M. Kalsin*[a]

Novel half-sandwich 18ē and 16ē arene ruthenium iminophosphonamide complexes [(η^6-C$_6$Me$_6$)RuCl{(R′N)$_2$PR$_2$}] (**3a–c**) and [(η^6-C$_6$Me$_6$)Ru{(R′N)$_2$PR$_2$}]$^+$(X$^-$) (**4a–c** (**a**, R = Ph, R′ = *p*-Tol; **b**, R = Et, R′ = *p*-Tol; **c**, R = Ph, R′ = Me. X = BF$_4$, PF$_6$ or BAr$^F_4$) were synthesized. The elongated Ru–Cl bond in the 18ē complexes is shown to dissociate even in apolar solvents to form the corresponding 16ē cations, which can be readily isolated as salts with non-coordinating anions. The coordinatively unsaturated 16ē complexes are stable species due to efficient π-electron donation from the nitrogen atoms of the zwitterionic NPN-ligand. The ruthenium iminophosphonamides are moderately active in the ROMP polymerization of norbornene; the 16ē complexes **4a,b** yield high molecular weight polymers ($M_n \sim 300 \times 10^3$) with a narrow distribution $M_w/M_n \sim 1.6$, while the 18ē complexes **3a,b** give polymers of lower molecular weight ($M_n < 50 \times 10^3$) with a wider polydispersity index $M_w/M_n \sim 2.5$.

Introduction

Among transition metal complexes with κ^2-*N,N*-heteroallylic ligands, the iminophosphonamides bearing a coordinated R$_2$P(NR′)$_2^-$ anion (NPN) are studied fragmentarily; there have been less than a hundred of molecular structures of NPN complexes established to date, that is in sharp contrast to more than a thousand of transition metal amidinate structures, according to the Cambridge Structural Database (CSD). The IV group metals,[1–6] chromium,[7–10] nickel[11–15] and copper[16–22] iminophosphonamides are the most studied, which is due to their catalytic application in cyclopropanation,[16,21,23] olefin oligomerization[7–9] and polymerization.[2,6,12,15,24,25] A few platinum metal group iminophosphonamides have been reported for palladium[24] and ruthenium[26] before 2009, when we started systematic studies of these complexes. We have demonstrated experimentally from the precision X-ray data by determining the deformational electron density for the palladium complex [Pd{(*p*-^{i}PrC$_6$H$_4$N)$_2$PPh$_2$}$_2$] that the iminophosphonamide ligand is zwitterionic N$^-$–P$^+$–N$^-$ having single P–N bonds and bearing full negative charges at the nitrogen atoms.[27] This result shows a big difference between the electronic properties of iminophosphonamide and amidinate complexes, which previously have been considered as having a similar heteroallylic delocalized π-electronic system. The HOMO orbital of the zwitterionic NPN ligand may have either C_{2v} or C_s symmetry,[28] of which the latter can efficiently donate the π-electron density from the nitrogen atoms to the d$_{xz}$-orbital of the metal located in the plane of the ligand, similarly to the β-diketiminate complexes (Chart 1A and B). In contrast, the C_{2v} symmetry of the HOMO orbital in the amidinate ligand allows π-donation only by lateral coordination of the amidinate ligand resulting in a strong folding of the four-membered metallacycle (Chart 1C).

Indeed, the electron deficient ruthenium complexes can be stabilized by intramolecular π-coordination of the amidinate ligand, which leads to strong puckering of the Ru–N–C–N metallacycle in the 16ē complexes [(Cp*)Ru{(^{t}BuN)$_2$C(Mes)}][29] and [(C$_6$Me$_6$)Ru{(^{i}PrN)$_2$CMe}][30] to 39.9° and 31.5°, respectively. The lateral coordination of the amidinate ligand stabilizes these 16ē complexes inefficiently since it weakens the M–N σ-bonds; such species are very reactive and can readily coordinate 2ē donors[30–32] or other organometallic moieties to form dinuclear μ^2-amidinate complexes.[33] At the same time, the solely reported ruthenium iminophosphonamide, the stable 16ē [(*p*-cymene)Ru{(^{i}PrN)$_2$PPh(NH^{i}Pr)}](BPh$_4$), did not react either with [Et$_3$NH]Cl, [PPh$_4$]Cl or with triphenylphosphine and triphenyl phosphite to form 18ē adducts; only carbon monoxide or cyanide could coordinate, however the corres-

[a] A.N. Nesmeyanov Institute of Organoelement Compounds, Russian Academy of Sciences, 28 Vavilov str., 119991 Moscow, Russia. E-mail: kalsin@ineos.ac.ru

[b] Laboratory of Macromolecular Chemistry and Organic Catalysis, Department of Chemistry, University of Liège, Sart-Tilman (B6a), 4000 Liège, Belgium

†Electronic supplementary information (ESI) available: Variable-temperature ^{1}H NMR of **3b** in toluene and the $\Delta G^{\neq}$ calculations for the exchange of *Et*$_a$ and *Et*$_b$ in **3b** in CD$_2$Cl$_2$. CCDC 1475876–1475879, 1494098 and 1494099. For ESI and crystallographic data in CIF or other electronic format see DOI: 10.1039/c6dt03202h
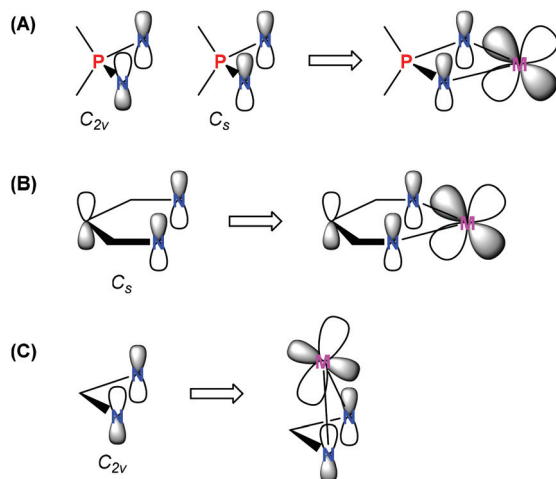
Chart 1 Schematic drawing of the HOMO orbitals of (A) iminophosphonamide, (B) β-diketiminate, and (C) amidinate ligands (on the left) and possible π-bonding with the d-orbital of the metal (on the right).

ponding 18ē complexes were not isolated.[26] For this complex the authors proposed a possibility of pseudo π-allyl donation to ruthenium based on a slight puckering of the Ru–N–P–N plane by 13.9°. Since that time the chemistry of ruthenium iminophosphonamides has not progressed, although two structures of 18ē [(p-cymene)RuBr{(p-TolN)$_2$PMe(p-TolNH)}] and 17ē [(Cp*)RuCl{(p-TolN)$_2$PMe(p-TolNH)}] complexes were deposited in CSD in 2004–2005 but their synthesis and properties were not published.

Recently, an interesting arene ruthenium bis(phosphinimino)methanide complex [(p-cymene)Ru(L)Cl] (L = PhN(PPh$_2$)CH(PPh$_2$)NPh) has been shown to exist as a cationic 18ē complex with a tridentate κ^3-C,N,N ligand L.[34] Although this ligand closely relates to iminophosphonamides, the stabilization of the 16ē species occurs by intramolecular coordination of the methanide group but not by the unpaired electron density from the nitrogen atoms. Indeed the displacement of the methanide group by Cl$^-$ or MeCN is highly unfavorable with the ΔG°_{298} calculated for the latter reaction to be +19 kcal mol^{-1}. This complex fails to react with CO under ambient conditions, which has also been attributed to the high nucleophilicity of the methanide group and the weak π-basicity of the ruthenium center.[35]

Here we report the synthesis of a series of new 18ē and 16ē half-sandwich arene ruthenium complexes with various iminophosphonamide ligands distinguished by the electronic properties of their N- and P-substituents, their physico-chemical and structural data in comparison to other κ^2-N,N-heteroallylic arene ruthenium complexes, and preliminary catalytic data for the ring-opening metathesis polymerization (ROMP) of norbornene.

Results and discussion

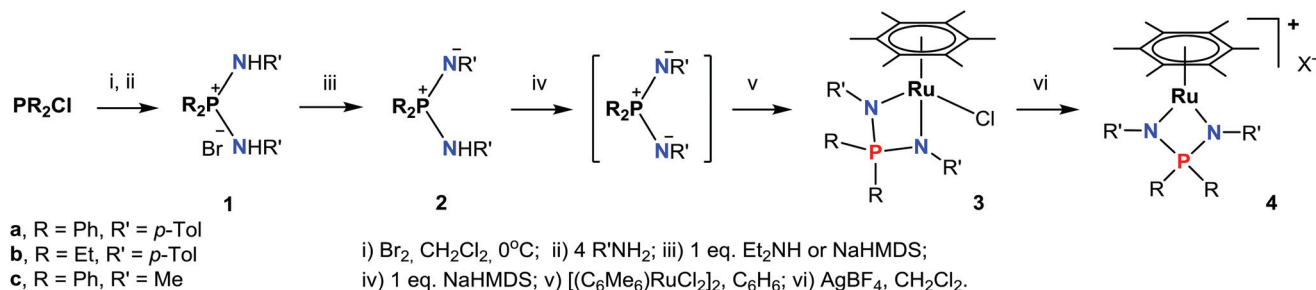### Synthesis and characterization of the complexes 3–4

The synthesis of arene ruthenium NPN-complexes (3–4) from the diaminophosphonium salts 1a–c is summarized in Scheme 1.

The diaminophosphonium salts [R$_2$P(NHR′)$_2$]Br (1a–c) were prepared in high yields, according to the earlier developed procedure.[36] The salts 1a–c can be monodeprotonated with strong bases like NaHMDS or n-BuLi to give the corresponding iminophosphonamines 2a–c, while the more acidic 1a is deprotonated easily with an equimolar amount of Et$_2$NH to yield 2a quantitatively. At the same time, NaHMDS is preferred for the synthesis of 2b and 2c; when n-BuLi is employed, the isolation of these iminophosphonamines is very laborious due to their complexation with lithium salts. The new compounds 1b and 2a,b were fully characterized spectroscopically and by elemental analysis, while we were not able to obtain satisfactory elemental analysis for 2c due to its high moisture sensitivity. In ^{31}P NMR the phosphorus signals of 2a–c are shifted by 27–32 ppm to less positive values compared to those of 1a–c. In ^{1}H NMR, the NH hydrogen of 1a (δ 9.26) is more acidic than the NH groups of 1b (δ 8.77) and 1c (δ 6.61) thus reflecting the electron-releasing effect of the N- and P-substituents on the electron density at the nitrogen atoms. Expectedly, the basic NH resonances of the iminophosphonamines 2a (δ 5.55) and 2b (δ 3.85) are shifted to less positive values. The signals from chemically inequivalent substituents at the nitrogen atoms in iminophosphonamines 2a,b are averaged tentatively due to intermolecular N–H···N proton exchange;[37] perhaps such exchange is responsible for not observing the NH signal for 2c.

Further deprotonation of 2a–c with 1 equiv. of NaHMDS results in the formation of sodium iminophosphonamides Na[R$_2$P(NR′)$_2$], as indicated by the new signals in ^{31}P NMR at more positive values δ 7.0 (R = Ph, R′ = p-Tol), δ 29.0 (R = Et, R′ = p-Tol) and δ 28.5 (R = Ph, R′ = Me) with respect to the corresponding iminophosphonamines 2a–c;[14,27,38] however they were not isolated due to extremely high moisture sensitivity. The iminophosphonamides Na[R$_2$P(NR′)$_2$] generated in situ react with the dimeric ruthenium complex [(η^6-C$_6$Me$_6$)RuCl$_2$]$_2$ to give the corresponding 18ē arene ruthenium(II) complexes 3a–c with the chelating bidentate NPN-ligand in moderate-to-high isolated yields (62–86%). The chloride ligand in 3a–c was easily replaced with the non-coordinating anions (PF$_6^-$, BF$_4^-$, BArF$_4$) by treating them with the corresponding silver or sodium salts in dichloromethane to afford the new 16ē cationic complexes [(η^6-C$_6$Me$_6$)Ru{(p-TolN)$_2$PPh$_2$}](PF$_6$) (4a), [(η^6-C$_6$Me$_6$)Ru{(p-TolN)$_2$PEt$_2$}](BF$_4$) (4b) and [(η^6-C$_6$Me$_6$)Ru{(MeN)$_2$PPh$_2$}](BArF$_4$) (4c) in nearly quantitative yields as deep-violet solids. All the complexes obtained were fully characterized by NMR spectroscopy and elemental analysis and their molecular structures were confirmed by single crystal X-ray diffraction studies. The selected structural parameters of 3a–c and 4a–c are given in Table 1 and their projections are shown in Fig. 1–6.

The 18ē complexes 3a–c exhibit a three-legged piano stool geometry with a pseudo-octahedral configuration of the ligands around the ruthenium atom. The Ru–C$_6$Me$_6$ (centroid) distance is in the range of 1.675(3)–1.662(4) Å, which is typical of neutral half-sandwich arene ruthenium complexes. Similarly to the β-diketiminate arene ruthenium complex,[39] in both 3a,b the C–C bond lengths in the η^6-coordinated arene noticeably alternate: the bonds C(2)–C(3), C(4)–C(5), and C(1)–C(6), which are

Scheme 1 Synthesis of complexes **3–4**.

a, R = Ph, R' = p-Tol
b, R = Et, R' = p-Tol
c, R = Ph, R' = Me

i) Br$_2$, CH$_2$Cl$_2$, 0 °C; ii) 4 R'NH$_2$; iii) 1 eq. Et$_2$NH or NaHMDS;
iv) 1 eq. NaHMDS; v) [(C$_6$Me$_6$)RuCl$_2$]$_2$, C$_6$H$_6$; vi) AgBF$_4$, CH$_2$Cl$_2$.

Table 1 Selected geometrical parameters of complexes **3a–c** and **4a–c**: the distances (Å), angles and dihedrals (°)

|	3a	3b	3c	4a	4b	4c
Ru···C$_6$Me$_6$(centroid)	1.675(3)	1.666(2)	1.662(4)	1.662(2)	1.675(1)	1.652(4)
Ru–C(arene)	2.175–2.233(3)	2.171–2.217(2)	2.159–2.218(4)	2.149–2.252(2)	2.143–2.275(1)	2.142–2.208(4)
Ru–N$_1$	2.137(2)	2.151(2)	2.137(4)	2.017(2)	2.0119(11)	2.011(4)
Ru–N$_2$	2.171(2)	2.161(2)	2.159(4)	2.036(2)	2.0733(10)	2.020(3)
P–N$_1$	1.600(2)	1.603(2)	1.605(4)	1.623(2)	1.6352(10)	1.615(4)
P–N$_2$	1.613(3)	1.615(2)	1.602(4)	1.624(2)	1.6233(10)	1.619(4)
Ru–Cl	2.438(3)	2.437(2)	2.445(4)			
N$_1$–Ru–N$_2$	68.08(9)	68.08(7)	69.39(14)	72.33(9)	72.17(4)	72.93(14)
N$_1$–P–N$_2$	97.30(12)	97.22(10)	99.36(19)	94.87(12)	95.22(5)	95.57(18)
Ru–N$_1$–P	97.98(11)	96.81(9)	95.94(18)	96.54(11)	94.82(5)	95.50(17)
Ru–N$_2$–P	96.25(11)	96.07(9)	95.15(17)	95.81(11)	97.56(5)	95.01(17)
Ru–N(1)–N(2)–P	173.69(15)	166.25(12)	175.9(3)	173.23(15)	175.02(6)	169.7(2)
C$_6$Me$_6$(centroid)–Ru–P	142.2	148.7	148.2	176.0	174.1	175.6
Ru–C(1)–C(4)/Ru–N(1)–N(2)				6.3	5.7	26.1
$\sum$(N$_1$)^a	359.2(5)	354.5(4)	357.6(8)	360.0(5)	359.8(2)	359.0(8)
$\sum$(N$_2$)^a	358.6(5)	354.6(4)	344.4(8)	354.9(5)	360.0(2)	356.9(8)

^{a} The sum of bond angles at the corresponding nitrogen atom.
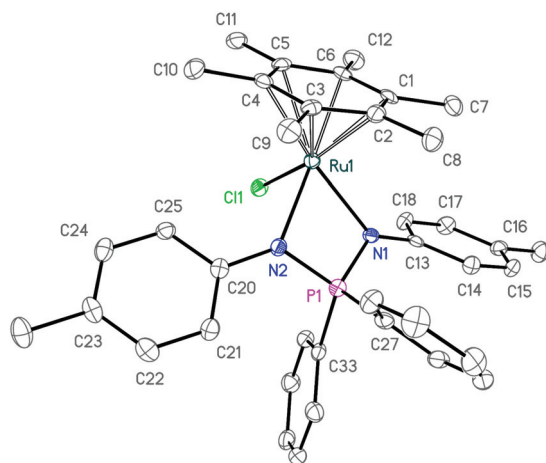
Fig. 1 ORTEP diagram of complex **3a**. Ellipsoids are shown at 50% probability, hydrogen atoms are omitted for clarity.
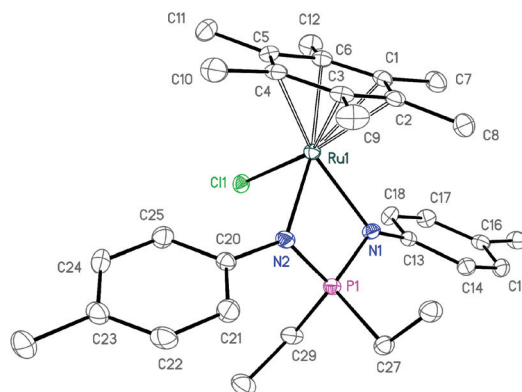

Fig. 2 ORTEP diagram of complex **3b**. Ellipsoids are shown at 50% probability, hydrogen atoms are omitted for clarity.

trans to the N(1), N(2) and Cl(1), are shorter (1.412–1.421 Å for **3a** and 1.417–1.423 Å for **3b**) than the bonds C(1)–C(2), C(3)–C(4), and C(5)–C(6) (1.436–1.442 Å for **3a** and 1.442–1.447 Å for **3b**). In contrast to this, in **3c** the coordinated arene gives a nearly eclipsed conformation with the chloride and the NPN-

ligands; only N(1) significantly deviates from that (the torsion angle N(1)–Ru–C$_6$Me$_6$(centroid)–C(1) is 18.5°), which results in shortening of the C(4)–C(5) bond *trans* to N(1) (1.417 Å), while the other C–C bonds are slightly longer (1.428–1.441 Å).

In iminophosphonamide complexes **3a–c** the Ru–N bonds (2.137–2.171 Å) and the Ru–Cl bonds (2.437–2.445 Å) are considerably longer than those in analogous 18ē arene ruthenium
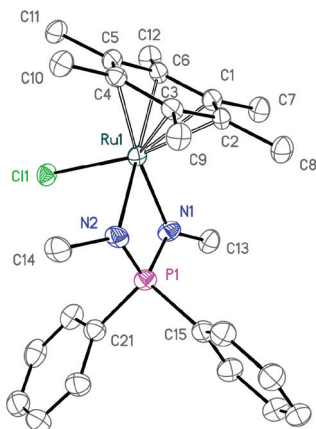
Fig. 3 ORTEP diagram of complex **3c**. Ellipsoids are shown at 50% probability, hydrogen atoms are omitted for clarity.
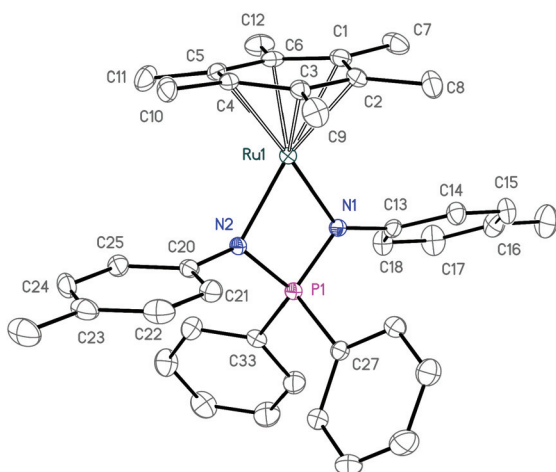

Fig. 4 ORTEP diagram of cation **4a**. Ellipsoids are shown at 50% probability, hydrogen atoms and the anion are omitted for clarity.
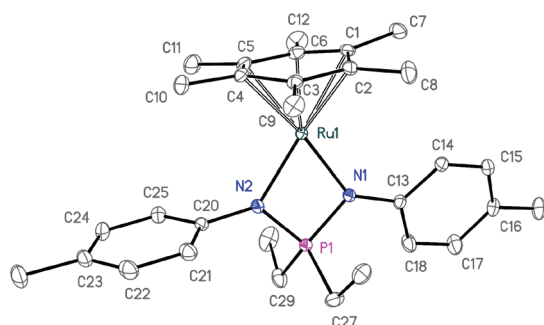

Fig. 5 ORTEP diagram of cation **4b**. Ellipsoids are shown at 50% probability, hydrogens atoms and the anion are omitted for clarity.
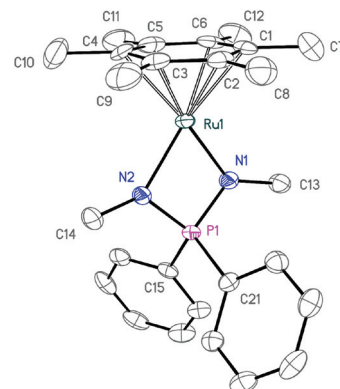

Fig. 6 ORTEP diagram of the cation **4c**. Ellipsoids are shown at 50% probability, hydrogen atoms and the anion are omitted for clarity.

bond is elongated in arene ruthenium complexes with highly efficient σ,π-donating β-diketiminate (2.461–2.521 Å)[39,46,47] or dianionic bis(imidazolin-2-iminate) (2.4853(4) Å) ligands,[48] up to full dissociation in the latter example.

The chlorine atom has intramolecular close CH⋯Cl contacts with one *ortho*-hydrogen (H18A) of the *N*-tolyl substituents. The H18A⋯Cl distances in **3a** (2.762 Å) and **3b** (2.813 Å) fall below the sum of the van der Waals radii of 2.95 Å (ref. 49 and 50) and the corresponding angles Cl⋯H–C of 140.4° (**3a**) and 140.8° (**3b**) are typical of such a type of non-directed interaction. The chlorine atom is almost coplanar to the plane of the tolyl ring involved in the H⋯Cl contact and the corresponding torsion angle Cl–H(18A)–C(18)–C(13) is 7.6° and 8.4° for **3a** and **3b**, respectively. A few other intra- and intermolecular close contacts H⋯Cl are observed in **3a,b** with the hydrogens of the C_6Me_6 ligand (the Cl⋯H11C, Cl⋯H11B distances are 2.772, 2.749 Å in **3a** and the Cl⋯H11C, Cl⋯H8A are 2.899, 2.871 Å in **3b**) and of the *P*-substituent (the Cl⋯H34A is 2.868 Å in **3a** and the Cl⋯H29A is 2.812 Å in **3b**). Similar intra- and intermolecular close contacts can be seen in **3c** between the chlorine atom and the hydrogen atoms of the methyl group at N(2) (Cl⋯H14B is 2.872 Å) and C_6Me_6 (Cl⋯H10C is 2.840 Å), respectively.

The chelate angle N(1)–Ru–N(2) in **3a–c** (68.1–69.4°) is significantly larger than that in the analogous 18ē ruthenium amidinate complexes (61–62°),[40–43,51] since the P–N bonds are longer than the corresponding C–N bonds in the amidinates. It is worth noting that the torsion angle Ru–N(1)–N(2)–P is close to 180° showing small puckering of the Ru–N(1)–P–N(2) metallacycle from the planarity (6.3° for **3a**, 13.7° for **3b** and 4.1° for **3c**). The pyramidalization of the nitrogen atoms is rather small in **3a,b**, while it is strong for one of the nitrogens in **3c**, for which the sum of the angles at the N(2) atom ∑(N) is 344.4°. Recently, a much wider range of puckering angles (up to 23.4°) and relatively strong pyramidalization of one of the nitrogen atoms (348–351°) were observed in the square-planar palladium iminophosphonamide complexes, presumably as a result of steric repulsion between the *N*-cumyl substituents of the NPN- and co-ligands.[27] However this seems to be not the

amidinate (2.078–2.139 Å and 2.400–2.434 Å, respectively)[40–44] or triazenide (2.104–2.133 Å and 2.386–2.397 Å)[45] complexes, perhaps due to the high negative charge located at the nitrogen atoms of the zwitterionic NPN-ligand. Indeed, the Ru–Cl

case of **3c** bearing sterically small *N*-methyl groups; more probably the pyramidalization of N(2) is due to the high unpaired electron density located fully at the nitrogen atom and being not able to delocalize on any other electron system like aromatic *N*-tolyl groups in **3a,b**.

The 16ē cationic complexes **4a–c** expectedly exhibit a two-legged piano-stool geometry with the chelating NPN-ligand positioned nearly perpendicular to the C_6Me_6 ring; the C_6Me_6 (centroid)–Ru–P angle is 174–176°. The Ru–C_6Me_6 (centroid) distance is 1.652–1.675 Å and is similar to that in **3a–c**. The Ru–N bond lengths in **4a–c** (2.011–2.073 Å) are close to those in [(*p*-cymene)Ru{(^iPrN)_2PPh(NH^iPr)}](BPh_4) (**5**) (2.011, 2.017 Å)[26] and are significantly shorter than in **3a–c** due to stronger binding with the positively charged ruthenium atom. Slightly shorter Ru–N distances were reported for 16ē cationic β-diketiminates (1.994–1.997 Å)[39] and bis(imidazolin-2-iminates) (1.977–2.003 Å),[48] while in the analogous ruthenium amidinate complexes these bonds are longer (2.058–2.065 Å),[30,32] showing the intermediate donating ability of the NPN-ligand. The C_6Me_6 ring is not planar but is significantly distorted towards the boat conformation making four Ru–C(arene) bonds shorter (2.149–2.178(2) Å in **4a** and 2.143–2.199(1) Å in **4b**) and two bonds, namely Ru–C(1) and Ru–C(4) (2.238(2), 2.252(2) Å for **4a** and 2.228(1), 2.275(1) Å for **4b**), longer. Unlike in the 18ē complexes **3a,b**, the C–C bonds in C_6Me_6 in **4a,b** do not alternate, instead the bonds C(2)–C(3) and C(5)–C(6) (1.440–1.444 Å) are slightly longer than the other four C–C bonds (1.418–1.428 Å) as a result of the stronger bonding of these carbons with the ruthenium atom. Importantly, in **4a,b** the longer Ru–C(1) and Ru–C(4) bonds are always *trans* to the Ru–N bonds (the dihedral angle between the planes Ru–C(1)–C(4) and Ru–N(1)–N(2) is 5.7–6.3°) with the longest Ru–C(4) bond *trans* to the shortest Ru–N(2) bond. A similar distortion of the coordinated arene planarity and the Ru–C(arene) bond distribution was earlier observed for **5**[26] and dicationic arene ruthenium complexes with the bis(imidazolin-2-imine) ligand.[48] It should be noted that in **4c** the arene and the NPN-ligand are in a staggered conformation (the dihedral angle between the planes Ru–C(2)–C(5) and Ru–N(1)–N(2) is 86.1°), which leads to slight shortening of the Ru–C(2) and Ru–C(5) (2.142(4), 2.163(4) Å) compared to the other four Ru–C(arene) bonds (2.177–2.208 Å) resulting in a flipped boat conformation of the arene.

The chelate angle N(1)–Ru–N(2) in **4a–c** (72.1–72.9°) is almost equal to that in **5** (71.8°)[26] and larger by *ca*. 4° than in **3a–c**. The pyramidalization of the nitrogen atoms ($\sum$(N) is 355–360°) and the puckering of the plane Ru(1)N(1)P(1)N(2) (5.0–10.3°) are small. This is in sharp contrast to the strong puckering (31.4°) of the chelate metallacycle M–N–C–N in the analogous amidinate 16ē arene ruthenium complex [(η^6-C_6Me_6)Ru{(N^iPr)_2CMe}](PF_6), required for additional stabilization of the coordinatively unsaturated species by a π-heteroallyl system.[30]

The structural peculiarities of the coordinated arene, the flattened RuNPN metallacycle and the short Ru–N bonds in **4a–c** are indicative of the strong σ,π-bonding of the iminopho-

sphonamide ligand[26] *via* nitrogen atoms, similarly to β-diketiminates and bis(imidazolin-2-iminates), and in contrast to allylic π-stabilization in metal amidinates. The elongated Ru–Cl bonds in **3a–c** and the pyramidalization of the nitrogen atom in the most electron-rich **3c** are also in agreement with the zwitterionic structure of the NPN ligand bearing enhanced negative charges at the nitrogen atoms.

In the ^{31}P NMR spectra of **3a,b** the phosphorus resonance (δ 43.9 for **3a** and δ 72.4 for **3b**) is shifted by *ca*. 47–49 ppm to more positive values compared to the precursors **2a** and **2b**. Interestingly, in the ^1H NMR spectra of **3a** and **3b** in $CDCl_3$ the two chemically inequivalent substituents at the phosphorus atom give only one set of signals for phenyl and ethyl groups, respectively. However, in the ^1H NMR spectra recorded in apolar C_6D_6, the *P*-substituents of **3a** and **3b** give rise to two sets of the corresponding resonances. Similarly, in the ^{13}C NMR spectra of **3a** and **3b** in $CDCl_3$ the resonances for only one type of phenyl and ethyl groups are observed. It is noteworthy that in ^{13}C NMR the characteristic doublets for *ipso*-carbons of phenyls are not found, perhaps due to their strong broadening. Apparently, in polar solvents fast exchange between the two *P*-substituents takes place. Indeed, heating a solution of **3a** and **3b** in apolar toluene-d_8 (*T* = 273–353 K) leads to broadening of the inequivalent phenyl and ethyl resonances, respectively for **3a** and **3b**, in ^1H NMR, though their coalescence is not achieved (see the ESI†). In a more polar CD_2Cl_2 solution of **3b** at 298 K the signals for only one ethyl substituent are observed, while decreasing the temperature to 193 K gives two separate resonances of methyl groups (Fig. 7). At the coalescence temperature of T_c = 238 K in dichloromethane, the estimated exchange rate constant is 1370 s^{-1} and the free energy of activation $\Delta G^{\neq}$ calculated from the Eyring equation is about 10.4 kcal mol^{-1}.[52]

The exchange between the *P*-substituents R_a and R_b seems to proceed *via* a C_{2v}-symmetric intermediate or a transition state with two equivalent R groups, tentatively the cationic complex [(η^6-C_6Me_6)Ru{R_2P(N-*p*-Tol)_2}]$^+$Cl$^-$ (*vide infra*), formed from **3a,b** by dissociation of the chloride anion (Scheme 2).

Although the dissociation of the chloride anion in 18ē complexes **3a,b** is facile in $CDCl_3$ or CD_2Cl_2, the equilibrium concentration of the dissociated 16ē form is negligible, as far as their signals in ^{31}P NMR in $CDCl_3$ (δ 43.9 for **3a**, δ 72.4 for **3b**) and C_6D_6 (δ 43.3 for **3a**, δ 71.1 for **3b**) remain virtually unchanged. The phosphorus resonance of the 16ē cationic complexes **4a** (δ 71.9) and **4b** (δ 102.3) is strongly shifted by ~30 ppm to more positive values compared to the neutral complexes **3a,b**. In the ^1H and ^{13}C NMR spectra of **4a,b** in CD_2Cl_2 the *P*-substituents are chemically equivalent, independent of the temperature (193–298 K) as it is expected for C_{2v}-symmetric complexes.

In apolar C_6D_6 complex **3c** also gives rise to two inequivalent phenyl groups in the ^1H and ^{13}C NMR spectra, which is consistent with the non-dissociated 18ē chloride complex, though the signals are broadened. Whereas in more polar $CDCl_3$ complex **3c** has violet color and its ^{31}P resonance (δ 76.9) is strongly shifted to more positive values than in C_6D_6 (δ 59.8) and becomes close to the signal of the cationic
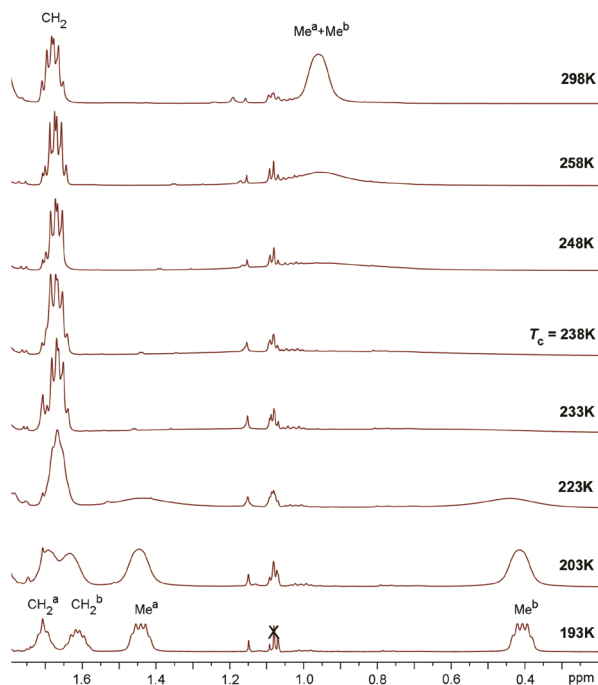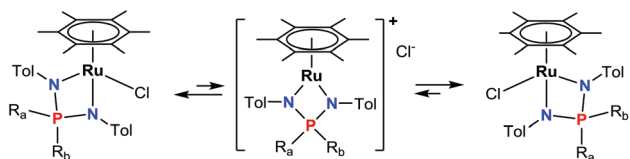
Fig. 7 VT NMR spectra of complex **3b** recorded in CD$_2$Cl$_2$ at T = 193–298 K (x – stands for grease).

Scheme 2 The exchange between R$_a$ and R$_b$ substituents *via* putative dissociation–association of the chloride anion.[53]

complex **4c** (δ 80.8). The ^{1}H NMR spectra of **3c** and **4c** in CDCl$_3$ are nearly identical and in line with the cationic C_{2v}-symmetric complex. Hence, in sharp contrast to **3a,b**, in CDCl$_3$ solution **3c** undergoes facile dissociation to give the cationic complex $[(\eta^6\text{-}C_6Me_6)Ru\{Ph_2P(NMe)_2\}]^+Cl^-$, which is prevalent in the equilibrium mixture. Apparently strongly electron-releasing *N*-methyl substituents enhance the π-donating ability of the NPN-ligand compared to that of the complexes **3a,b** bearing weaker *N*-tolyl donors.

The arene ruthenium complexes having monoanionic β-diketiminate[39] and dianionic bis(imidazolin-2-iminate)[48] ligands have also been reported earlier to undergo facile chloride dissociation, whereas in the amidinate ruthenium complexes the counter-ion dissociation has been observed only for the weakly coordinating triflate ligand but not the chloride.[51] Hence the capability of the iminophosphonamide ligand to donate electrons and to stabilize the electron-deficient states is much higher than that of the amidinate ligand and comparable to the β-diketiminate and zwitterionic bis(imidazolin-2-iminate) ligands.
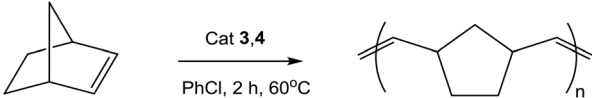
In the UV-vis spectra the complexes **4a–c** have a broad medium intensity band at λ_{max} 540–550 nm shifted to lower energies compared to the corresponding complexes **3a,b** (in CH$_2$Cl$_2$) and **3c** (in C$_6$H$_6$) having a band at λ_{max} 410–450 nm. Similar bands at λ_{max} 520–530 nm have also been observed for 16ē pentamethylcyclopentadienyl amidinate,[29] β-diketiminate[47] and bis(imidazolin-2-iminate)[48] ruthenium complexes, which has been attributed to d–d centered transitions.[47]

The 16ē complexes **4a–c** are remarkably stable in solution to air and moisture in sharp contrast to the 18ē complexes **3a–c**, which hydrolyze to produce the corresponding phosphinoxides R$_2$P(O)(NHR′). Apparently the nitrogen atoms in **3a–c** are highly basic due to their free electron pairs and thus are prone to the attack by water molecules, whereas in **4a–c** these electron pairs participate in π-bonding to the ruthenium atom and are much less basic. Indeed, the susceptibility to hydrolysis is higher for the complex bearing more electron-releasing *N*-substituents; thus **3c** decomposes within minutes in wet CD$_2$Cl$_2$ while **3a,b** are stable for hours. Under similar conditions **4a–c** do not hydrolyze and do not form the 18ē aqua NPN-complexes; their NMR spectra in dried and wet solvents are the same and remain unchanged for days. However, when 10 equivalents of MeCN were added to a solution of **4a** in CD$_2$Cl$_2$ the colour immediately changed from violet to red and the phosphorus resonance shifted from δ 72.2 to δ 63.8 indicating the formation of the new complex, presumably the cationic adduct $[(\eta^6\text{-}C_6Me_6)Ru(MeCN)\{Ph_2P(N\text{-}p\text{-}Tol)_2\}](PF_6)$. The attempt to isolate it by removing the excess of acetonitrile *in vacuo* returned the starting complex **4a** (violet solution in CD$_2$Cl$_2$ with the phosphorus resonance at δ 71.0, no acetonitrile signal in ^{1}H NMR). Bubbling carbon monoxide into a solution of **4a** in CH$_2$Cl$_2$ leads to the formation of a yellow CO adduct (ν_{CO} = 1984 cm^{-1}), however the CO ligand is labile and easily decoordinates upon removing the solvent under reduced pressure to give back **4a**. A similar 16ē ruthenium iminophosphonamide **5** has also been recently reported to coordinate reversibly CO to form the unstable CO adduct (ν_{CO} = 1993 cm^{-1}) and to not react with Cl$^-$, PPh$_3$, and P(OPh)$_3$.[26] In sharp contrast, the more electron-deficient arene ruthenium amidinate $[(\eta^6\text{-}C_6H_6)$Ru$\{PhC(N^tBu)_2\}](BAr^F_4)$ readily forms the stable carbonyl complex $[(\eta^6\text{-}C_6H_6)Ru(CO)\{PhC(N^tBu)_2\}](BAr^F_4)$, in which the CO band is observed at a much higher frequency (ν_{CO} = 2050 cm^{-1}).[30] On the other hand, the carbonyl band in the arene ruthenium complex with the dianionic dithiolate ligand $[(\eta^6\text{-}C_6Me_6)Ru(CO)(SXyl)_2]$ (ν_{CO} = 1965 cm^{-1})[54] is close to that in the CO adduct of the iminophosphonamide **4a** and hence indirectly evidences for the zwitterionic nature of the NPN-ligand. Apparently in cationic iminophosphonamides **4a–c** the positive charge is predominantly located on the phosphorus atom rather than on the ruthenium atom and thus their electronic properties are more like those of neutral arene ruthenium complexes with dianionic ligands.

ROMP polymerization of norbornene

Half-sandwich arene ruthenium complexes with sterically bulky phosphanes have been shown earlier to be readily acces-

Table 2 Experimental data for the ring-opening metathesis polymerization of norbornene catalyzed by complexes **3–4**[a]

Entry	Complex	Monomer conv. (%)	Polymer yield (%)	M_n (kg mol^{-1})	M_w/M_n
1	**3a**	87	76	50	2.7
2	**3b**	93	82	36	2.5
3	**3c**	59	51	40	6.9
4	**4a**	91	70	283	1.65
5	**4b**	98	79	341	1.55
6	**4c**	10	6	—	—

[a] Norbornene (7.5 mmol); catalyst (0.03 mmol); TMSD (0.1 mmol); chlorobenzene (30 mL); 2 h at 60 °C under argon.

sible precatalysts for ring-opening metathesis polymerization of both strained (norbornene) and low-strain (cyclooctene) cycloolefins and their functionalized derivatives.[55,56] Typically, the polymers obtained from norbornene had a number-average molecular weight M_n of $60–80 \times 10^3$ and a molecular weight distribution M_w/M_n of 1.6. We have demonstrated that under the same catalytic conditions the complexes **3a–c** and **4a,b** activated by trimethylsilyldiazomethane (TMSD) catalyze the polymerization of norbornene, except for almost inactive **4c** (Table 2).

The 18ē complexes **3a–c** produced polymers of low molecular weight $M_n = 36–50 \times 10^3$, which is close to the expected $M_n = 23.5 \times 10^3$ calculated from the catalyst/substrate ratio (1/250), meaning that all ruthenium centers are involved in catalysis. The molecular weight distribution is relatively wide: M_w/M_n is 2.5–2.7 for **3a,b** and is 6.9 for **3c**. The polydispersity of the polymer can be significantly improved when 16ē complexes **4a,b** are employed. They yield polymers of a much higher molecular weight $M_n = 283–341 \times 10^3$, which is supposedly due to their limited solubility in chlorobenzene and hence only a minor fraction (about 10%) of these cationic complexes can participate in the catalytic cycle. This assumption would mean that the actual activity of **4a,b** is about ten times higher than that of **3a,b**. Both types of complexes give a considerable fraction (11–20%) of low-weight oligomers soluble in methanol.

In the absence of TMSD the ruthenium iminophosphonamides studied are inactive. The actual catalytically active species in the ROMP of olefins are carbene complexes, which are typically generated *in situ* from the precatalysts and TMSD. Recently, the 16ē cationic ruthenium amidinate complexes have been reported to react with TMSD to result in migration of the SiMe3 group to the ruthenium atom and formation of the amidinato-carbene complexes, in which the carbene moiety is inserted into the RuNCN metallacycle.[57] These amidinate complexes provided low activity in the ROMP polymerization of norbornene; higher activity was mentioned for polymerization of high-strain norbornadiene catalyzed by the 18ē complex [[(C6H6)RuBr{MeC(N^{i}Pr)2}] although the detailed results were not published.[32] Perhaps, a similar carbene inser-

tion into the Ru–N bond occurs in the NPN-precatalysts.[58] Not surprisingly, the more electron rich iminophosphonamide arene ruthenium complexes **3a,b** and **4a,b** excel the corresponding ruthenium amidinates in the ROMP polymerization of norbornene. However, our attempts to involve them in the ROMP of low-strain cyclooctene were unsuccessful.

It is noteworthy that strongly electron-releasing *N*-methyl substituents drastically decrease the activity of the complexes **3c** and **4c**. The negligible activity of the 16ē complex **4c** could be a result of very efficient stabilization of the unsaturated ruthenium center to make it insusceptible to the reaction with the generated *in situ* carbene CHSiMe3 rather than of the solubility issues. The same can be attributed to the reduced activity of **3c**, which should partially dissociate in polar chlorobenzene to form stable 16ē cationic species (*vide supra*).

Experimental

General procedures

All manipulations were carried out using standard Schlenk techniques under an atmosphere of dry argon. Solvents were purified by standard methods and distilled prior to use. Ph2PCl and Et2PCl were distilled under high vacuum or at ambient pressure, respectively, prior to use; other commercially available compounds were used as received. ^{1}H, ^{31}P and ^{13}C NMR spectra were obtained on a Bruker AMX-400 spectrometer and referenced to the residual signals of deuterated solvent (^{1}H and ^{13}C), and to 85% H3PO4 (^{31}P, external standard). Elemental analyses were performed on a Carlo Erba 1106 CHN analyzer. The following compounds were prepared according to described procedures: [Ph2P(NH-*p*-Tol)2]Br (**1a**),[36] [(η^6-C6Me6)RuCl2]2,[59] Na[B(3,5-C6H3(CF3)2)4] (NaBAr^{F}4).[60]

Synthesis of [Et2P(NH-*p*-Tol)2]Br (1b). To a solution of Et2PCl (2.67 g, 21.5 mmol) in CH2Cl2 (30 mL) cooled to 0 °C a solution of Br2 (1.10 mL, 21.5 mmol) in CH2Cl2 (30 mL) was added dropwise. The reaction mixture was warmed to 20 °C, stirred for 1.5 h and cooled again to 0 °C. A solution of *p*-toluidine (9.2 g, 86 mmol) in CH2Cl2 (50 mL) was added to the reaction mixture and the resulting suspension was stirred over-

night at 20 °C. The precipitate was filtered off and washed with CH_2Cl_2 (3 × 20 mL). The filtrate was evaporated to dryness and the oily product was stirred with ethyl acetate (150 mL) for 2 h. The fine crystal formed was filtered off, washed with ethyl acetate (3 × 10 mL) and dried *in vacuo* to yield 5.80 g of **1b**. The filtrate was concentrated to 30 mL and left overnight. The precipitated crystal was filtered off, washed with ethyl acetate (3 × 3 mL) and dried *in vacuo* to give additionally 0.92 g of the product. The total yield was 6.72 g (82%). Anal. calcd for $C_{18}H_{26}BrN_2P$: C, 56.70; H, 6.87; N, 7.35%. Found: C, 56.92; H, 6.96; N, 7.33%. ^{31}P NMR ($CDCl_3$): δ 50.4. ^{1}H NMR ($CDCl_3$): δ 8.77 (d, $^{2}J_{HP}$ = 13.6, 2H, NH), 7.28 (d, ^{3}J = 8.0, 4H, C_6H_4), 6.85 (d, ^{3}J = 8.0, 4H, C_6H_4), 2.62 (dq, $^{3}J_{HP}$ = 14.0, ^{3}J = 7.6, 4H, CH_2CH_3), 2.15 (s, 6H, Me_{Tol}), 1.04 (dt, $^{4}J_{HP}$ = 21.1, ^{3}J = 7.6, 6H, CH_2CH_3). ^{13}C NMR ($CDCl_3$): δ 135.6 (br. s, i-C_{Tol}(N)), 133.3 (s, i-C_{Tol}(Me)), 130.1 (s, β-C_{Tol}), 119.7 (br. s, α-C_{Tol}), 20.6 (s, Me_{Tol}), 14.7 (d, $^{1}J_{CP}$ = 80, CH_2Me), 4.8 (s, CH_2Me).

Synthesis of [$Ph_2P(NHMe)_2$]Br (1c). To a solution of Ph_2PCl (4.35 mL, 24.0 mmol) in CH_2Cl_2 (50 mL) at room temperature a solution of Br_2 (1.23 mL, 24.0 mmol) in CH_2Cl_2 (15 mL) was added dropwise. The reaction mixture was stirred for 1.5 h and cooled to −50 °C. A freshly prepared cold solution of dimethylamine in CH_2Cl_2 (3 M, 75 mL, 225 mmol) was added to the reaction mixture and the resulting suspension was stirred overnight at 20 °C. The precipitate was filtered off and washed with CH_2Cl_2 (3 × 40 mL). The filtrate was evaporated to dryness and then washed with benzene (5 × 20 mL) and acetone (5 × 20 mL). The white crystalline residue was dried *in vacuo* to yield 6.25 g of **1c** (80%). Anal. calcd for $C_{14}H_{18}BrN_2P$: C, 51.71; H, 5.58; N, 8.61%. Found: C, 51.89; H, 5.74; N, 8.69%. ^{31}P NMR ($CDCl_3$): δ 40.2. ^{1}H NMR ($CDCl_3$): δ 7.97 (dd, $^{3}J_{HP}$ = 13.0, ^{3}J = 8.2, 4H, o-H_{Ph}), 7.51 (dt, ^{3}J = 7.6, $^{5}J_{HP}$ = 1.0, 2H, p-H_{Ph}), 7.40 (dt, ^{3}J = 8.0, $^{4}J_{HP}$ = 3.6, 4H, m-H_{Ph}), 6.61 (dq, $^{2}J_{HP}$ = 16.2, ^{3}J = 5.4, 1H, NH), 2.57 (dd, $^{3}J_{HP}$ = 13.0, ^{3}J = 5.4, 6H, NMe). ^{13}C NMR ($CDCl_3$): δ 123.0 (d, ^{1}J = 126.0, i-C_{Ph}), 132.4 (d, ^{2}J = 11.2, o-C_{Ph}), 129.5 (d, ^{3}J = 13.7, m-C_{Ph}), 133.9 (d, ^{4}J = 2.7, p-C_{Ph}), 26.1 (s, NMe).

Synthesis of [$Ph_2P(N$-p-$Tol)(NH$-p-$Tol)$] (2a). To a suspension of **1a** (2.00 g, 4.19 mmol) in benzene (50 mL) at room temperature neat Et_2NH (0.45 mL, 4.35 mmol) was added. The mixture was stirred for 4 h. The fine microcrystal was filtered off, washed with benzene (2 × 20 mL) and discarded. The filtrate was evaporated to dryness, and the residue was washed with 10 mL of Et_2O/hexane = 1/2 (v : v). Finally, it was redissolved in benzene; the hazy solution was filtered to remove the traces of the ammonium salts and then evaporated to give off-white powder. Yield 1.62 g (97%). Anal. calcd for $C_{26}H_{25}N_2P$: C, 78.77; H, 6.36; N, 7.06%. Found: C, 78.94; H, 6.49; N, 6.95%. ^{31}P NMR ($CDCl_3$): δ −3.5. ^{1}H NMR ($CDCl_3$): δ 7.93 (ddd, $^{3}J_{HP}$ = 12.4, ^{3}J = 8.1, ^{4}J = 1.8, 4H, o-H_{Ph}), 7.39–7.51 (m, 6H, m,p-H_{Ph}), 6.96 (d, ^{3}J = 7.5, 4H, C_6H_4), 6.92 (d, ^{3}J = 7.5, 4H, C_6H_4), 5.55 (br. s, 1H, NH), 2.21 (s, 6H, CH_3). ^{13}C NMR (C_6D_6): δ 132.7 (d, ^{1}J = 130.6, i-C_{Ph}), 132.2 (d, ^{2}J = 9.1, o-C_{Ph}), 131.3 (s, p-C_{Ph}), 129.8 (s, β-C_{Tol}), 128.9 (br. s, i-C_{Tol}(Me)), 128.5 (d, ^{3}J = 12.9, m-C_{Ph}), 121.3 (br. d, ^{3}J = 11.8, α-C_{Tol}), 20.5 (s, Me_{Tol}).

Synthesis of [$Et_2P(N$-p-$Tol)(NH$-p-$Tol)$] (2b). To a solution of **1b** (0.76 g, 2.0 mmol) in benzene (30 mL) at room temperature a 2.0 M solution of NaHMDS (1.0 mL, 2.0 mmol) in THF was added and the mixture was stirred for 2 h. The precipitate of NaBr was filtered off and washed with benzene (3 × 5 mL). The filtrate was evaporated to dryness and the oily residue was washed with hexane (2 × 3 mL) to give quantitatively the product. For an analytical purity the product was recrystallized from warm diethyl ether. Yield 0.55 g (92%). Anal. calcd for $C_{18}H_{25}N_2P$: C, 71.97; H, 8.39; N, 9.33%. Found: C, 71.95; H, 8.41; N, 9.27%. ^{31}P NMR ($CDCl_3$): δ 23.3. ^{1}H NMR ($CDCl_3$): δ 6.96 (br. s, 8H, C_6H_4), 3.85 (br. s, 1H, NH), 2.24 (s, 6H, CH_3), 2.07 (dq, $^{2}J_{HP}$ = 14.4, ^{3}J = 7.6, 4H, CH_2CH_3), 1.12 (dt, $^{3}J_{HP}$ = 18.5, ^{3}J = 7.6, 6H, CH_2CH_3). ^{13}C NMR (C_6D_6): δ 144.5 (br. s, i-C_{Tol}(N)), 128.6 (s, i-C_{Tol}(Me)), 129.9 (s, β-C_{Tol}), 121.1 (d, $^{3}J_{CP}$ = 12, α-C_{Tol}), 20.5 (s, Me_{Tol}), 18.9 (d, $^{1}J_{CP}$ = 87, CH_2Me), 6.4 (d, $^{2}J_{CP}$ = 3, CH_2Me).

Synthesis of [$Ph_2P(NMe)(NHMe)$] (2c). To a suspension of **1c** (1.00 g, 3.05 mmol) in THF (50 mL) at room temperature a 2.0 M solution of NaHMDS (1.5 mL, 3.0 mmol) in THF was added and the mixture was stirred for 18 h. The precipitate of NaBr was filtered off and washed with THF (3 × 5 mL). The filtrate was evaporated to dryness and the oily residue was washed with hexane (2 × 3 mL) and dried *in vacuo* to give a colorless glassy solid. Yield 0.72 g (96%). ^{31}P NMR ($CDCl_3$): δ 12.4. ^{1}H NMR (THF-d_8): δ 7.95 (ddd, $^{3}J_{HP}$ = 11.2, ^{3}J = 7.6, ^{4}J = 2.0, 4H, o-H_{Ph}), 7.45–7.52 (m, 6H, m,p-H_{Ph}), 2.81 (d, $^{3}J_{HP}$ = 18.0, 6H, CH_3).

Synthesis of [(η^6-C_6Me_6)RuCl{$R_2P(N$-p-$Tol)_2$}] (3a,b). General procedure. To a solution of **2a** (0.80 g, 2.02 mmol) in benzene (60 mL) a 2.0 M solution of NaHMDS in THF (1.10 mL, 2.20 mmol) was added and the resulting solution was stirred for 1 h. Then the solid [(η^6-C_6Me_6)RuCl$_2$]$_2$ (0.67 g, 1.00 mmol) was added and the reaction mixture was stirred overnight. The solvent was removed *in vacuo*, the residue was washed with hexane (2 × 10 mL) and extracted with CH_2Cl_2 (100 mL). The filtrate was diluted with 10 mL of benzene and slowly evaporated to 3–5 mL. The precipitated brick-red crystal was filtered off, washed with benzene (2 mL), Et_2O (10 mL) and dried under vacuum. Yield 1.20 g (86%). Anal. calcd for $C_{38}H_{42}ClN_2PRu$: C, 65.74; H, 6.10%. Found: C, 65.87; H, 6.29%. ^{31}P NMR ($CDCl_3$): δ 43.9. ^{1}H NMR ($CDCl_3$): δ 7.76 (br. dd, $^{3}J_{HP}$ = 12, ^{3}J = 8, 4H, o-H_{Ph}), 7.44 (br. t, 2H, p-H_{Ph}), 7.33 (br. m, 4H, m-H_{Ph}), 6.88 (d, ^{3}J = 8.0, 4H, C_6H_4), 6.78 (d, ^{3}J = 8.0, 4H, C_6H_4), 2.10 (s, 6H, Me_{Tol}), 1.95 (s, 18H, C_6Me_6). ^{1}H NMR (C_6D_6): δ 8.07 (m, 2H, o-H_{Ph}), 7.91 (ddd, $^{3}J_{HP}$ = 11.2, ^{3}J = 8.0, ^{3}J = 1.6, 2H, o'-H_{Ph}), 7.35 (dd, ^{3}J = 8.0, $^{4}J_{HP}$ = 1.2, 4H, C_6H_4), 7.23 (m, 3H, (p' + m)-H_{Ph}), 6.89 (d, ^{3}J = 8.0, 4H, C_6H_4), 6.73 (m, 3H, (p + m')-H_{Ph}), 2.10 (s, 6H, Me_{Tol}), 1.80 (s, 18H, C_6Me_6). ^{13}C NMR ($CDCl_3$): δ 144.6 (d, $^{2}J_{CP}$ = 4.4, i-C_{Tol}(N)), 133.2 (d, $^{2}J_{CP}$ = 10.9, o-C_{Ph}), 131.4 (d, $^{4}J_{CP}$ = 2.0, p-C_{Ph}), 128.5 (s, β-C_{Tol}), 127.9 (s, i-C_{Tol}(Me)), 127.6 (d, $^{3}J_{CP}$ = 12.7, m-C_{Ph}), 125.1 (d, ^{3}J = 9.3, α-C_{Tol}), 89.2 (s, C_6Me_6), 20.5 (s, Me_{Tol}), 16.2 (s, C_6Me_6). UV-vis (CH_2Cl_2; λ_{max}, nm; ε, M^{-1} cm^{-1}): 450 (900).

Analogously, from **2b** (0.51 g, 1.70 mmol) in THF (50 mL), NaHMDS (2.0 M, 0.90 ml, 1.80 mmol) and [(η^6-C_6Me_6)RuCl$_2$]$_2$

(0.56 g, 0.85 mmol), complex **3b** was obtained. The product was purified by precipitation from a benzene solution (3–5 mL) with hexane (10–15 mL) and further recrystallized from Et$_2$O. Yield 0.74 g (73%). Anal. calcd for C$_{30}$H$_{42}$ClN$_2$PRu: C, 60.24; H, 7.08%. Found: C, 60.37; H, 7.11%. ^{31}P NMR (CDCl$_3$): δ 72.4. ^{1}H NMR (CDCl$_3$): δ 7.04 (d, ^3J = 8.0, 4H, C$_6$H$_4$), 6.89 (d, ^3J = 8.0, 4H, C$_6$H$_4$), 2.23 (s, 6H, Me$_{Tol}$), 1.89 (s, 18H, C$_6$Me$_6$), 1.77 (dq, $^2J_{HP}$ = 11.7, ^3J = 7.6, 4H, CH$_2$CH$_3$), 1.05 (dt, $^3J_{HP}$ = 16.2, ^3J = 7.6, 6H, CH$_2$CH$_3$). ^{1}H NMR (C$_6$D$_6$): δ 7.48 (d, ^3J = 7.7, 4H, C$_6$H$_4$), 7.11 (d, ^3J = 7.7, 4H, C$_6$H$_4$), 2.33 (s, 6H, Me$_{Tol}$), 2.17 (br. dq, $^2J_{HP}$ = 14.4, ^3J = 7.8, 2H, CH$_2'$CH$_3$), 1.86 (s, 18H, C$_6$Me$_6$), 1.47 (br. dt, $^3J_{HP}$ = 15.6, ^3J = 7.2, 3H, CH$_2$CH$_3$), 1.31 (br. dq, $^2J_{HP}$ = 14.4, ^3J = 7.2, 2H, CH$_2$CH$_3$), 0.54 (br. dt, $^3J_{HP}$ = 15.6, ^3J = 7.8, 3H, CH$_2$CH$_3'$). ^{13}C NMR (CDCl$_3$): δ 145.1 (d, $^2J_{CP}$ = 4.0, i-C$_{Tol}$(N)), 128.9 (s, i-C$_{Tol}$(Me)), 128.8 (s, β-C$_{Tol}$), 126.1 (d, $^3J_{CP}$ = 6.7, α-C$_{Tol}$), 88.7 (s, C$_6$Me$_6$), 25.7 (d, $^1J_{CP}$ = 54.8, CH$_2$Me), 20.6 (s, Me$_{Tol}$), 15.9 (s, C$_6$Me$_6$), 6.5 (d, $^2J_{CP}$ = 4.8, CH$_2$Me). UV-vis (CH$_2$Cl$_2$; λ$_{max}$, nm; ε, M^{-1} cm^{-1}): 450 (940).

Synthesis of [(η^6-C$_6$Me$_6$)RuCl{Ph$_2$P(NMe)$_2$}] (3c). To a solution of **1c** (0.76 g, 2.3 mmol) in THF (50 mL) a 2.0 M solution of NaHMDS in THF (1.20 mL, 2.40 mmol) was added and the resulting solution was stirred for 3 h. The precipitate of NaBr was removed by filtration, the filtrate was treated again with a 2.0 M solution of NaHMDS (1.2 mL, 2.4 mmol) and stirred for an extra 3 h. Then the solid [(η^6-C$_6$Me$_6$)RuCl$_2$]$_2$ (0.77 g, 1.15 mmol) was added and the reaction mixture was stirred overnight. The solvent was removed *in vacuo*, and the residue was washed with hexane (2 × 10 mL) and extracted with benzene (40 mL). The filtrate was diluted with 40 mL of hexane, and the flocculated black impurities were filtered off. The solution was evaporated to 5–7 mL and set for crystallization in a fridge at −20 °C. The precipitated dark-red crystalline was filtered off, washed with cold hexane (5 mL) and dried under vacuum. Yield 0.77 g (62%). Anal. calcd for C$_{26}$H$_{34}$ClN$_2$PRu: C, 57.61; H, 6.32%. Found: C, 57.40; H, 6.38%. ^{31}P NMR (C$_6$D$_6$): δ 59.8. ^{31}P NMR (CDCl$_3$): δ 76.9. ^{1}H NMR (C$_6$D$_6$): δ 8.00 (br. s, 2H, o-H$_{Ph}$), 7.69 (br. s, 2H, o-H$_{Ph}$), 7.21 (br. s, 3H, (m + p)-H$_{Ph}$), 7.12 (br. s, 1H, p'-H$_{Ph}$), 7.05 (br. s, 2H, m'-H$_{Ph}$), 2.74 (d, $^3J_{HP}$ = 19.2, 6H, NMe), 1.84 (s, 18H, C$_6$Me$_6$). ^{1}H NMR (CDCl$_3$): δ 7.55 (td, ^3J = 7.2, $^5J_{HP}$ = 1.2, 2H, p-H$_{Ph}$), 7.44 (td, ^3J = 8.0, $^4J_{HP}$ = 2.8, 4H, m-H$_{Ph}$), 7.26 (dd, $^3J_{HP}$ = 10.4, ^3J = 8.0, 4H, o-H$_{Ph}$), 2.71 (d, $^3J_{HP}$ = 19.2, 6H, NMe), 2.27 (s, 18H, C$_6$Me$_6$). ^{13}C NMR (C$_6$D$_6$): δ 140.6 (d, $^1J_{CP}$ = 104.0, i-C$_{Ph}$), 132.2 (d, $^1J_{CP}$ = 58.2, i-C$_{Ph'}$), 134.9 (br. s, o-C$_{Ph}$), 131.3 (br. s, p-C$_{Ph}$), 130.5 (br. s, (m + m')-C$_{Ph}$), 130.2 (br. s, (o' + p')-C$_{Ph}$), 88.7 (s, C$_6$Me$_6$), 32.9 (s, NMe), 15.6 (s, C$_6$Me$_6$). UV-vis (toluene; λ$_{max}$, nm; ε, M^{-1} cm^{-1}): 410 (1550).

Synthesis of [(η^6-C$_6$Me$_6$)Ru{R$_2$P(N-p-Tol)$_2$}](X) (4a, X = PF$_6$; 4b, X = BF$_4$; 4c, X = BAr$^F_4$). General procedure. (a) To a solution of **3a** (0.46 g, 0.66 mmol) in CH$_2$Cl$_2$ (30 ml), solid AgPF$_6$ (0.18 g, 0.72 mmol) was added, the color immediately changed from red to deep violet. The reaction mixture was stirred for 3 h and then filtered through a plug of Celite. The solution was concentrated to 2 mL, further addition of Et$_2$O (10 mL) resulted in the precipitation of a product, which was filtered off, washed with Et$_2$O (2 × 5 mL) and dried under vacuum.

Yield of **4a** 0.51 g (96%). Anal. calcd for C$_{38}$H$_{42}$F$_6$N$_2$P$_2$Ru: C, 56.78; H, 5.27%. Found: C, 56.69; H, 5.12%. ^{31}P NMR (CDCl$_3$): 71.9, −144.4 (sept, J_{PF} = 707, PF$_6^-$). ^{1}H NMR (CDCl$_3$): δ 7.64 (td, ^3J = 7.6, $^5J_{HP}$ = 1.2, 2H, p-H$_{Ph}$), 7.49 (td, ^3J = 7.6, $^4J_{HP}$ = 3.2, 4H, m-H$_{Ph}$), 7.38 (dd, $^3J_{HP}$ = 12.0, ^3J = 7.2, 4H, o-H$_{Ph}$), 7.02 (d, ^3J = 7.6, 4H, C$_6$H$_4$), 6.68 (d, ^3J = 7.6, 4H, C$_6$H$_4$), 2.28 (s, 6H, Me$_{Tol}$), 2.08 (s, 18H, C$_6$Me$_6$). ^{13}C NMR (CD$_2$Cl$_2$): δ 141.6 (d, $^2J_{CP}$ = 2, i-C$_{Tol}$(N)), 135.3 (s, i-C$_{Tol}$(Me)), 134.2 (d, $^4J_{CP}$ = 2.3, p-C$_{Ph}$), 132.0 (d, $^2J_{CP}$ = 10.6, o-C$_{Ph}$), 130.1 (s, β-C$_{Tol}$), 129.3 (d, $^3J_{CP}$ = 12.4, m-C$_{Ph}$), 126.3 (d, ^3J = 6.2, α-C$_{Tol}$), 126.2 (d, ^1J = 90.5, i-C$_{Ph}$), 89.9 (s, C$_6$Me$_6$), 20.8 (s, Me$_{Tol}$), 16.5 (s, C$_6$Me$_6$). UV-vis (CH$_2$Cl$_2$; λ$_{max}$, nm; ε, M^{-1} cm^{-1}): 540 (1320).

Analogously, from **3b** (0.45 g, 0.75 mmol) and AgBF$_4$ (0.15 g, 0.77 mmol), complex **4b** was obtained (0.46 g, 93%). Anal. calcd for C$_{30}$H$_{42}$BF$_4$N$_2$PRu: C, 55.48; H, 6.52%. Found: C, 55.61; H, 6.44%. ^{31}P NMR (CDCl$_3$): δ 102.3. ^{1}H NMR (CDCl$_3$): δ 7.14 (d, ^3J = 6.0, 4H, C$_6$H$_4$), 6.91 (d, ^3J = 6.0, 4H, C$_6$H$_4$), 2.31 (s, 6H, Me$_{Tol}$), 2.02 (s, 18H, C$_6$Me$_6$), 1.59 (br. dq, $^2J_{HP}$ = 10, ^3J = 8, 4H, CH$_2$CH$_3$), 0.99 (br. dt, $^3J_{HP}$ = 16, ^3J = 8, 6H, CH$_2$CH$_3$). ^{13}C NMR (CDCl$_3$): δ 141.4 (d, $^2J_{CP}$ = 4.0, i-C$_{Tol}$(N)), 134.9 (d, $^5J_{CP}$ = 2.0, i-C$_{Tol}$(Me)), 130.3 (s, β-C$_{Tol}$), 125.7 (d, $^3J_{CP}$ = 5.2, α-C$_{Tol}$), 89.2 (s, C$_6$Me$_6$), 20.6 (s, Me$_{Tol}$), 19.8 (d, $^1J_{CP}$ = 53.6, CH$_2$Me), 16.3 (s, C$_6$Me$_6$), 5.2 (d, $^2J_{CP}$ = 5.4, CH$_2$Me). UV-vis (CH$_2$Cl$_2$; λ$_{max}$, nm; ε, M^{-1} cm^{-1}): 540 (1410).

Analogously, from **3c** (0.14 g, 0.26 mmol) and NaBAr$^F_4$ (0.23 g, 0.27 mmol), complex **4c** was obtained (0.34 g, 96%). Anal. calcd for C$_{58}$H$_{46}$BF$_{24}$N$_2$PRu: C, 50.86; H, 3.38%. Found: C, 50.85; H, 3.34%. ^{31}P NMR (CDCl$_3$): δ 80.8. ^{1}H NMR (CDCl$_3$): δ 7.71 (br. s., 8H, o-H$_{BARF}$), 7.60 (ttd, ^3J = 7.5, ^4J = 1.5, $^5J_{HP}$ = 1.4, 2H, p-H$_{Ph}$), 7.50 (br. s., 4H, p-H$_{BARF}$), 7.46 (td, ^3J = 7.5, $^4J_{HP}$ = 3.0, 4H, m-H$_{Ph}$), 7.25 (dd, $^3J_{HP}$ = 12.9, ^3J = 7.2, 4H, o-H$_{Ph}$), 2.74 (d, $^3J_{HP}$ = 18.3, 6H, NMe), 2.27 (s, 18H, C$_6$Me$_6$). ^{13}C NMR (CDCl$_3$): δ 161.7 (q, $^1J_{CB}$ = 49.8, i-C$_B$(BAr^F)), 128.7 (qq, $^2J_{CF}$ = 31.2, $^3J_{CB}$ = 2.4, m-C(BAr^F)), 117.4 (m, o-C(BAr^F)), 134.7 (br. s, p-C(BAr^F)), 124.5 (q, $^1J_{CF}$ = 272.6, CF$_3$), 133.8 (d, $^4J_{CP}$ = 2.4, p-C$_{Ph}$), 131.1 (d, $^2J_{CP}$ = 9.9, o-C$_{Ph}$), 129.3 (d, $^3J_{CP}$ = 11.6, m-C$_{Ph}$), 124.9 (d, ^1J = 87.5, i-C$_{Ph}$), 89.3 (s, C$_6$Me$_6$), 33.2 (s, NMe), 16.4 (s, C$_6$Me$_6$). UV-vis (CH$_2$Cl$_2$; λ$_{max}$, nm; ε, M^{-1} cm^{-1}): 550 (1300).

Typical procedure for the ROMP of norbornene

A 50 mL round-bottom flask equipped with a magnetic stirring bar and capped with a three-way stopcock was charged with the ruthenium complexes **3–4** (0.03 mmol) and degassed chlorobenzene (20 mL) was added under an argon atmosphere. The solution was stirred for a few minutes at room temperature and then in an oil bath thermostated at 60 °C. Norbornene (1.5 M in chlorobenzene, 5 mL, 7.5 mmol) and eventually trimethylsilyldiazomethane, TMSD (0.1 M in a hexanes–chlorobenzene mixture, 1 mL, 0.1 mmol) were added with a syringe, and the reaction mixture was stirred for 2 h at 60 °C. The conversion was monitored by gas chromatography using norbornane as an internal standard. The resulting gel was diluted with CHCl$_3$ (20 mL) and slowly poured into MeOH (500 mL) under vigorous stirring. The precipitated polymer was filtered, dried under dynamic vacuum, and characterized

Table 3 Crystal data and structure refinement parameters for **3a–c** and **4a–c**

	3a	3b	3c	4a	4b	4c
Formula	$C_{38}H_{42}ClN_2PRu$	$C_{30}H_{42}ClN_2PRu$	$C_{26}H_{34}ClN_2PRu$	$C_{38}H_{42}F_6N_2P_2Ru$	$C_{30}H_{42}BF_4N_2PRu$	$C_{58}H_{46}BF_{24}N_2PRu$
Formula weight	694.22	598.14	542.04	803.74	649.50	1369.82
T, K	100	100	100	100	100	120
Crystal system	Monoclinic	Monoclinic	Triclinic	Monoclinic	Monoclinic	Monoclinic
Space group	$P2_1/n$	$P2_1/c$	$P\bar{1}$	$P2_1/n$	$C2/c$	$P2_1/c$
Z/Z'	4/1	4/1	2/1	4/1	8/1	4/1
a, Å	8.6451(9)	9.890(3)	8.8288(13)	9.7804(6)	25.9645(3)	12.2605(8)
b, Å	20.932(2)	36.718(9)	8.8550(13)	32.185(2)	9.96760(10)	28.9349(15)
c, Å	17.7244(19)	8.509(2)	16.886(3)	12.0350(8)	23.1951(3)	17.1266(10)
α, °			87.525(3)			
β, °	99.594(2)	113.639(7)	79.413(2)	107.2960(10)	96.5526(6)	108.197(2)
γ, °			68.626(2)			
V, Å^3	3162.6(6)	2830.4(13)	1208.0(3)	3617.1(4)	5963.76(12)	5771.9(6)
$d_{calc.}$, g cm^{-3}	1.458	1.404	1.490	1.476	1.447	1.576
μ, cm^{-1}	6.62	7.26	8.42	5.83	6.27	4.18
$2\theta_{max}$, °	54	60	54	60	60	56
Refls. collected/independent	32 206/6902	26 013/8183	16 106/5286	46 296/10 527	74 134/8695	41 189/13 856
Observed reflections $[I > 2\sigma(I)]$	4730	6453	4315	7940	8146	7865
R_1	0.0388	0.0385	0.0506	0.0461	0.0218	0.0653
wR_2	0.0670	0.0835	0.1262	0.1043	0.0641	0.1570
GOF	1.007	1.040	1.036	1.087	1.043	1.060
Residual density, e Å^{-3} (d_{max}/d_{min})	0.798/−0.735	0.761/−0.664	2.120/−0.945	1.526/−0.927	0.568/−0.509	1.277/−0.863

by NMR spectroscopy and GPC in THF using a polystyrene calibration.

X-ray crystal structure determination

Single crystals of **3** and **4** were obtained by slow diffusion of Et$_2$O to a solution of a complex (**3a**, **4a–c**) in CH$_2$Cl$_2$, or by diffusion of hexane to a solution of **3b** and **3c** in benzene. Data collection for all samples was performed on a Bruker SMART APEX II diffractometer (MoKα radiation, λ = 0.71073 Å) equipped with an Apex II CCD detector. Frames were integrated using the Bruker SAINT software package[61] by a narrow-frame algorithm. A semiempirical absorption correction was applied with the SADABS[62] program using the intensity data of equivalent reflections. The structures were solved with direct methods and refined by the full-matrix least-squares technique against F^2_{hkl} in anisotropic approximation with the SHELX[63] software package. The positions of hydrogen atoms were calculated, and all hydrogen atoms were refined in a riding model with $1.5U_{eq}(C_m)$ and $1.2U_{eq}(C_i)$, where $U_{eq}(C_m)$ and $1.2U_{eq}(C_i)$ are respectively the equivalent thermal parameters of the methyl and all other carbon atoms to which the corresponding H atoms are bonded. Detailed crystallographic information is given in Table 3. Crystallographic data have been deposited to the Cambridge Crystallographic Data Centre, CCDC numbers 1475876–1475879, 1494098 and 1494099.

18ē complexes **3a–c** as well as short Ru–N bonds in the 16ē complexes **4a–c** and small puckering of the Ru–N–P–N metalla-cycle indeed suggest the zwitterionic nature and strong σ,π-donor character of the iminophosphonamide ligand being able to donate 4ē or 6ē. Due to charge separation between the phosphorus and the nitrogen atoms, the electronic properties of the NPN-ligand are similar to those of dianionic ligands and therefore it can efficiently stabilize 16ē electron deficient complexes. Among other arene ruthenium complexes with κ^2-N,N chelating ligands, the properties of 16ē iminophosphonamide complexes resemble those of strongly donating monoanionic β-diketiminates and dianionic bis(imidazolin-2-iminates), and render them air stable unlike the analogous air-sensitive 16ē amidinate complexes. Thus arene ruthenium complexes **3a,b** and **4a,b** bearing the strongly donating NPN-ligand perform better than the analogous ruthenium amidinates in the ROMP of strained norbornene. To properly address the unusually low activity of complexes **3c**, **4c** with the most electron-rich NPN-ligand, which seems to block the activation of the ruthenium center by carbene, a deeper mechanistic investigation is required. The detailed kinetic and thermodynamic studies on the dissociation of the chlorides **3a–c** and the coordination of various ligands to their 16ē counterparts **4a–c** as well as the ROMP mechanistic study and application in the transfer hydrogenation of ketones are in progress and to be reported soon.

Conclusions

A series of new 18ē and 16ē hexamethylbenzene ruthenium complexes with the iminophosphonamide ligand have been synthesized and fully characterized. The elongated Ru–Cl bonds and an easy dissociation of the chloride anion in the

Acknowledgements

Notes and references

1 R. Vollmerhaus, R. Tomaszewski, P. Shao, N. J. Taylor, K. J. Wiacek, S. P. Lewis, A. Al-Humydi and S. Collins, *Organometallics*, 2005, **24**, 494–507.

2 R. Vollmerhaus, P. Shao, N. J. Taylor and S. Collins, *Organometallics*, 1999, **18**, 2731–2733.

3 M. Witt, M. Noltemeyer, H.-G. Schmidt, T. Lübben and H. W. Roesky, *J. Organomet. Chem.*, 1999, **591**, 138–147.

4 E. Müller, J. Müller, F. Olbrich, W. Brüser, W. Knapp, D. Abeln and F. T. Edelmann, *Eur. J. Inorg. Chem.*, 1998, **1998**, 87–91.

5 C. Qi and S. Zhang, *Appl. Organomet. Chem.*, 2006, **20**, 70–73.

6 R. Tomaszewski, R. Vollmerhaus, A. Al-Humydi, Q. Wang, N. J. Taylor and S. Collins, *Can. J. Chem.*, 2006, **84**, 214–224.

7 K. Albahily, V. Fomitcheva, S. Gambarotta, I. Korobkov, M. Murugesu and S. I. Gorelsky, *J. Am. Chem. Soc.*, 2011, **133**, 6380–6387.

8 K. Albahily, V. Fomitcheva, Y. Shaikh, E. Sebastiao, S. I. Gorelsky, S. Gambarotta, I. Korobkov and R. Duchateau, *Organometallics*, 2011, **30**, 4201–4210.

9 K. Albahily, S. Licciulli, S. Gambarotta, I. Korobkov, R. Chevalier, K. Schuhen and R. Duchateau, *Organometallics*, 2011, **30**, 3346–3352.

10 K. Albahily, Y. Shaikh, E. Sebastiao, S. Gambarotta, I. Korobkov and S. I. Gorelsky, *J. Am. Chem. Soc.*, 2011, **133**, 6388–6395.

11 R. Boese, M. Düppmann, W. Kuchen and W. Peters, *Z. Anorg. Allg. Chem.*, 1998, **624**, 837–845.

12 R. Schubbe, K. Angermund, G. Fink and R. Goddard, *Macromol. Chem. Phys.*, 1995, **196**, 467–478.

13 W.-J. Guo and Z.-X. Wang, *J. Org. Chem.*, 2013, **78**, 1054–1061.

14 B. Prashanth and S. Singh, *J. Chem. Sci.*, 2015, **127**, 315–325.

15 R. L. Stapleton, J. Chai, N. J. Taylor and S. Collins, *Organometallics*, 2006, **25**, 2514–2524.

16 I. V. Shishkov, F. Rominger and P. Hofmann, *Organometallics*, 2009, **28**, 1049–1059.

17 B. F. Straub, F. Eisenträger and P. Hofmann, *Chem. Commun.*, 1999, 2507–2508.

18 P. Hofmann, I. V. Shishkov and F. Rominger, *Inorg. Chem.*, 2008, **47**, 11755–11762.

19 B. F. Straub, F. Rominger and P. Hofmann, *Organometallics*, 2000, **19**, 4305–4309.

20 B. F. Straub, F. Rominger and P. Hofmann, *Chem. Commun.*, 2000, 1611–1612.

21 B. F. Straub, I. Gruber, F. Rominger and P. Hofmann, *J. Organomet. Chem.*, 2003, **684**, 124–143.

22 N. Nebra, C. Lescot, P. Dauban, S. Mallet-Ladeira, B. Martin-Vaca and D. Bourissou, *Eur. J. Org. Chem.*, 2013, 984–990.

23 B. F. Straub and P. Hofmann, *Angew. Chem., Int. Ed.*, 2001, **40**, 1288–1290.

24 W. Keim, R. Appel, A. Storeck, C. Krüger and R. Goddard, *Angew. Chem., Int. Ed.*, 1981, **20**, 116–117.

25 S. Collins, *Coord. Chem. Rev.*, 2011, **255**, 118–138.

26 P. J. Bailey, K. J. Grant and S. Parsons, *Organometallics*, 1998, **17**, 551–555.

27 T. A. Peganova, A. V. Valyaeva, A. M. Kalsin, P. V. Petrovskii, A. O. Borissova, K. A. Lyssenko and N. A. Ustynyuk, *Organometallics*, 2009, **28**, 3021–3028.

28 More correctly, Chart 1 shows the symmetry adapted linear combinations (SALC) of the atomic orbitals. The corresponding molecular orbitals retain the same symmetry elements, however their designation transforms either to A_2 and B_1 or A″ and A′, respectively for the planar or lateral coordination of the metal atom. Here we used the point group symmetries for SALC to be independent of the symmetry of the resulting complex.

29 H. Kondo, T. Sue, A. Kageyama, Y. Yamaguchi, Y. Sunada and H. Nagashima, *J. Organomet. Chem.*, 2009, **694**, 795–800.

30 T. Hayashida, Y. Yamaguchi, K. Kirchner and H. Nagashima, *Chem. Lett.*, 2001, 954–955.

31 Y. Yamaguchi and H. Nagashima, *Organometallics*, 2000, **19**, 725–727.

32 H. Nagashima, H. Kondo, T. Hayashida, Y. Yamaguchi, M. Gondo, S. Masuda, K. Miyazaki, K. Matsubara and K. Kirchner, *Coord. Chem. Rev.*, 2003, **245**, 177–190.

33 H. Kondo, Y. Yamaguchi and H. Nagashima, *J. Am. Chem. Soc.*, 2001, **123**, 500–501.

34 C. Bibal, M. Pink, Y. D. Smurnyy, J. Tomaszewski and K. G. Caulton, *J. Am. Chem. Soc.*, 2004, **126**, 2312–2313.

35 C. Bibal, Y. D. Smurnyy, M. Pink and K. G. Caulton, *J. Am. Chem. Soc.*, 2005, **127**, 8944–8945.

36 O. V. Gusev, T. A. Peganova, A. V. Gonchar, P. V. Petrovskii, K. A. Lyssenko and N. A. Ustynyuk, *Phosphorus, Sulfur Silicon Relat. Elem.*, 2009, **184**, 322–331.

37 O. J. Scherer and P. Klusmann, *Z. Anorg. Allg. Chem.*, 1969, **370**, 171.

38 M. Düppmann, W. Kuchen, W. Peters and W. Phosphorus, *Sulfur Silicon Relat. Elem.*, 1997, **129**, 53–58.

39 A. D. Phillips, G. Laurenczy, R. Scopelliti and P. J. Dyson, *Organometallics*, 2007, **26**, 1120–1122.

40 T. Singh, R. Kishan, M. Nethaji and N. Thirupathi, *Inorg. Chem.*, 2012, **51**, 157–169.

41 T. Hayashida and H. Nagashima, *Organometallics*, 2002, **21**, 3884–3888.

42 P. J. Bailey, L. A. Mitchell and S. Parsons, *J. Chem. Soc., Dalton Trans.*, 1996, 2839–2841.

43 W. W. Seidel, W. Dachtler and T. Pape, *Z. Anorg. Allg. Chem.*, 2012, **638**, 116–121.

44 I. J. Munslow, A. R. Wade, R. J. Deeth and P. Scott, *Chem. Commun.*, 2004, 2596–2597.

45 C. F. Barboza da Silva, S. Schwarz, M. Galceran Mestres, S. Teijelo López and J. Strähle, *Z. Anorg. Allg. Chem.*, 2004, **630**, 1919–1923.

46 A. D. Phillips, O. Zava, R. Scopelitti, A. A. Nazarov and P. J. Dyson, *Organometallics*, 2010, **29**, 417–427.

47 A. D. Phillips, K. Thommes, R. Scopelliti, C. Gandolfi, M. Albrecht, K. Severin, D. F. Schreiber and P. J. Dyson, *Organometallics*, 2011, **30**, 6119–6132.

48 T. Glöge, D. Petrovic, C. Hrib, P. G. Jones and M. Tamm, *Eur. J. Inorg. Chem.*, 2009, 4538–4546.

49 A. Bondi, *J. Phys. Chem.*, 1964, **68**, 441–451.

50 R. S. Rowland and R. Taylor, *J. Phys. Chem.*, 1996, **100**, 7384–7391.

51 T. Hayashida, H. Kondo, J. I. Terasawa, K. Kirchner, Y. Sunada and H. Nagashima, *J. Organomet. Chem.*, 2007, **692**, 382–394.

52 A. D. Bain, *Prog. Nucl. Magn. Reson. Spectrosc.*, 2003, **43**, 63–103.

53 Although we observe the formation of the cationic 16ē species in the solution of **3c** in chloroform or dichloromethane proving them to be possible intermediates, the actual exchange mechanism in apolar solvents can be more complicated or even different from the one given in the simplified Scheme 2.

54 K. Mashima, H. Kaneyoshi, S. Kaneko, A. Mikami, K. Tani and A. Nakamura, *Organometallics*, 1997, **16**, 1016–1025.

55 A. W. Stumpf, E. Saive, A. Demonceau and A. F. Noels, *J. Chem. Soc., Chem. Commun.*, 1995, 1127–1128.

56 A. Demonceau, A. W. Stumpf, E. Saive and A. F. Noels, *Macromolecules*, 1997, **30**, 3127–3136.

57 T. Hayashida and H. Nagashima, *Organometallics*, 2001, **20**, 4996–4998.

58 The model reaction of **4b** with 3 equiv. of TMSD in dichloromethane resulted in a complex mixture of products, one of each having the signal in ^{31}P NMR at δ 78.3 perhaps corresponds to a carbene complex (a characteristic doublet in ^{1}H NMR at δ 9.2 with $J_{H–P}$ = 16 Hz). To define the structures of all the species formed and their evolution with time in the ROMP catalytic cycle further mechanistic investigation is to be carried out.

59 M. Bennett, T. N. Huang, T. Matheson, A. Smith, S. Ittel and W. Nickerson, *Inorg. Synth.*, 1982, **21**, 74–78.

60 N. A. Yakelis and R. G. Bergman, *Organometallics*, 2005, **24**, 3579–3581.

61 Bruker, *SAINT v7.23A*, 2005.

62 G. M. Sheldrick, *SADABS v2008/1, Bruker/Siemens Area Detector Absorption Correction Program*, 2008.

63 G. M. Sheldrick, *Acta Crystallogr., Sect. C: Cryst. Struct. Commun.*, 2015, **71**, 3–8.